

1 Intensity modulated particle therapy for multiple targets

1.1 Introduction

Lung cancer is the leading cause of cancer-related death, with approximately 160 000 deaths in the U.S. in 2014 [Siegel et al., 2014]. More than half of all patients with lung cancer are diagnosed with stage IV non-small cell lung cancer (NSCLC) [Ramalingam and Belani, 2008, Iyengar et al., 2014]. Prognosis for stage IV NSCLC is poor, with only 12 months median survival after first line chemotherapy [Socinski et al., 2013].

Stereotactic body radiation treatment (SBRT) shows good results for treating NSCLC [Baumann et al., 2009, Fakiris et al., 2009, Grutters et al., 2010, Greco et al., 2011]. Furthermore, several studies have shown that SBRT can be used in the setting of limited metastatic disease [Rusthoven et al., 2009, Villaruz et al., 2012, Salama et al., 2012, Iyengar et al., 2014]. Passive scattering particle therapy has also proved as an effective treatment for NSCLC [Grutters et al., 2010, Tsujii and Kamada, 2012] and it could be considered an alternative to photon treatment.

It was shown in Chapter ?? that scanned carbon ions (PT) could also be used as a treatment modality for NSCLC. One of the conclusions of the study shown in Chapter ?? was that patients with multiple disease sites would especially benefit from PT compared to SBRT. However, limitations of this study were the small number of patients (4) and a single-field uniform optimization (SFUD) used in treatment planning. Several vital organs need to be considered in treatment planning for NSCLC patients, besides lungs, such as heart, spinal cord, esophagus and large vessels. Due to overlapping entry channels SFUD is limited in treating NSCLC, especially in patients with tumor in close vicinity to a vital organ. It is not possible to create clinically acceptable treatment plans with SFUD for such complex geometry.

We hypothesize that intensity modulated particle therapy (IMPT), permits to calculate adequate treatment plans. Furthermore, IMPT should provide single fraction scheme in patients, where SBRT was limited by OAR constraints.

Treatment of lung cancer patients with multiple disease sites was investigated with state of the art 4D IMPT optimization. Treatment plans were generated with two different 4D optimization techniques and compared with SBRT plans, which were actually used for treating patients.

1.2 Materials and Methods

The 4D extension of GSI's treatment planning system TRiP98 [Krämer and Scholz, 2000, Richter et al., 2013] was used and modified to create treatment plans. A description of modifications and tools used will be given here, alongside with patient data.

1.2.1 Patient data

In this study, 8 patients with 2 - 5 lung metastases summing to 24 metastases in total were included. The lesion size was 4.2 cm^3 (median, 25-75% 2.4 - 22.2) and peak-to-peak motion was 5.9 mm (2.7 - 8.1). Details are given in Table 1.1. Target motion and PT treatment planning were based on a 4D-CT, consisting of 10 phases (0 - 9), with phase 0 (end-inhale) chosen as a reference phase. A registered positron emission tomography (PET) scan was used to delineate clinical target volumes (CTV).

Patients 1 - 3 had no while patients 4 - 8 had at least one OAR in CTV vicinity (closer than 10 mm).

Patients were treated with SBRT at Chamaplimaud Center for the Unknown, Lisbon (Portugal), with different fraction schemes. Number of fractions and doses delivered are given in Table 1.1.

Table 1.1: Target characteristics, with CTV volumes, peak-to-peak motions, fractionation schemes and number of fields used for PT treatment planning. Last column shows an OAR in target vicinity (closer than 10 mm), if present. SA stands for smaller airways and esoph. for esophagus.

Patient	Target	Volume (cm ³)	Peak-to-peak motion [mm]	Fractionation scheme	Number of fields	OAR in proximity
1	a	10.2	3.4	1 x 24 Gy	2	
	b	14.4	2.8	1 x 24 Gy	2	
2	a	3.8	5.8	1 x 24 Gy	2	
	b	4.3	0.8	1 x 24 Gy	2	
	c	2.7	3.4	1 x 24 Gy	2	
	d	3.1	2.1	1 x 24 Gy	2	
	e	0.5	0.5	1 x 24 Gy	2	
3	a	139	0.6	1 x 24 Gy	3	
	b	9.2	2.0	1 x 24 Gy	2	
4	a	4	9	3 x 9 Gy	5	SA, esoph., heart
	b	0.8	7.8	1 x 24 Gy	2	
5	a	3.4	5	1 x 24 Gy	3	
	b	2.4	4.4	1 x 24 Gy	2	
	c	2.0	6.3	1 x 24 Gy	2	Heart
	d	2.4	6.4	1 x 24 Gy	2	Heart
6	a	20.6	7.4	1 x 24 Gy	4	SA
	b	27.1	6.0	1 x 24 Gy	5	SA
7	a	2.3	12	1 x 24 Gy	2	
	b	0.4	11.8	5 x 7 Gy	5	Heart, esoph., stomach
8	a	136	12	3 x 9 Gy	2	Heart
	b	12.4	2.5	1 x 20 Gy	2	
	c	123	14	3 x 9 Gy	2	Heart
	d	80.7	17	1 x 22 Gy	3	
	e	86.7	6.6	1 x 20 Gy	3	SA

1.2.2 Multiple targets

The TRiP98 optimization works on minimizing the residual of a nonlinear equation system [Krämer and Scholz, 2000]. The cost function $E(\vec{N})$ for particle number \vec{N} is:

$$E(\vec{N}) = \sum_{i \in T} \left(D_{plan}^i - D_{act}^i(\vec{N}) \right) + \theta(D_{act} - D_{max}) w_{OAR} \sum_{j \in OAR} \left(D_{act}^j(\vec{N}) - D_{Max} \right) \quad (1.1)$$

For a CT voxel i and j in target T and OAR, respectively; D_{plan} , D_{act} and D_{max} are the planned, actual and maximum allowed dose, respectively; θ is a Heaviside step function and w_{OAR} is an OAR specific weight.

The $D_{act}(\vec{N})$ is calculated as

$$D_{act}(\vec{N}) = \sum_{k=1}^n RBE(N) c_{ik} N \quad (1.2)$$

The coefficient c_{ik} gives the dose deposition at voxel i of a pencil beam k , with n being the number of pencil beams and RBE is relative biological effectiveness, calculated with the local effect model or LEM [Elsaesser et al., 2010] .

There is no restriction for the number of targets or fields in the minimizing function, so the first part of Eq. 1.1 can be expanded to:

$$E(\vec{N}) = \sum_T \sum_{i \in T} \left(D_{plan}^{i,T} - \sum_{k=1}^n c_{ik} N \right) \quad (1.3)$$

However, the setup of raster points in TRiP98 allowed only one target. It was therefore expanded in a way that a field was designated to a specific target, as displayed in Fig 1.1. Raster points for each field are created only around the designated target. All fields contribute dose to all voxels in optimization. Specifically, k in Eq. 1.3 runs over all pencil beams. Because the optimization function was not changed, all TRiP98 4D functionalities could be used, as explained in the next sections.

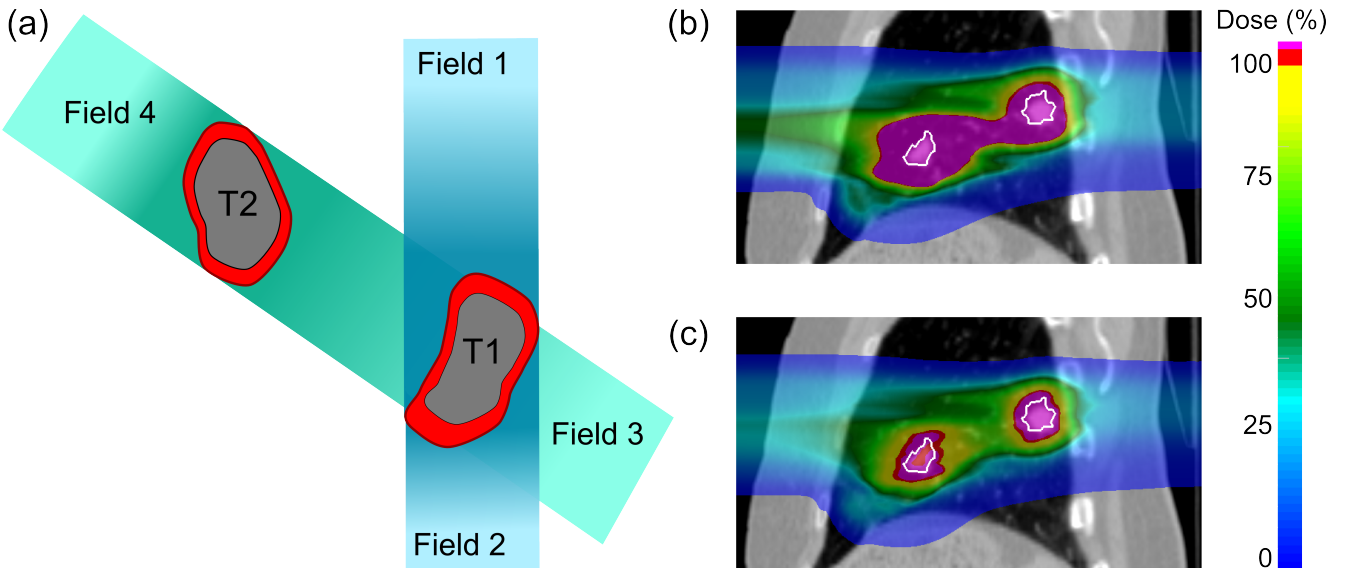


Figure 1.1: Optimization of multiple targets. (a) Fields 1 and 2 are designated to target T1 and fields 3 and 4 to target T2. Optimization takes into account all target voxels and contributions from all fields. An example is shown in (b) and (c), where targets were optimized individually (b) and together (c). The dose in (b) reaches almost 200% in healthy tissue.

1.2.3 Optimization techniques

Investigation of two different optimization techniques to handle range changes in moving tumors was made. For each patient, two sets of plans were created: a field-independent ITV (ITV) and a 4D optimization (4Dopt).

- **Field-independent ITV:** A water-equivalent path length ITV (WEPL-ITV) is different for each field, creating unnecessary margins when combining WEPL-ITV from different fields (see Fig. 1.2a). Graeff et. al [Graeff et al., 2012] proposed a solution to include range margins into the field description itself, instead of creating a bigger PTV.

Thus, all fields have the same target in optimization, permitting simultaneous optimization. Treatment plans were made for all targets with IMPT on a ITV in reference phase. Additionally target in motion state 5 (end-exhale) was included in optimization to make plan more robust against range changes in different motion states.

- **4D Optimization:** To include WEPL change specific to each motion state, a 4D optimization was used. 4Dopt uses a WEPL-ITV for raster setup, however the actual optimization is performed on each target voxel in each motion state m . The optimization function thus changes to [Graeff et al., 2012]:

$$E(\vec{N}) = \sum_{m=1}^M \sum_{T_m} \sum_{i \in T_m} \left(D_{plan}^i - \sum_{k=1}^n c_{ikm} N \right) \quad (1.4)$$

All targets were treated with IMPT and 4D optimization. Due to the large optimization problem for targets 3a - b, 5a - d, 6b, 8a and 8c, where targets had a big volume or OARs were included besides targets in optimization a subset of motion states was used [Graeff et al., 2012]. To cover most of the different tumor positions, two extreme motion states (0 and 5) and an intermediate position (7) were chosen.

The same number of fields and the same field angles were used in both techniques.

To reduce optimization problem, only portion of large OARs, such as heart or esophagus, were used. Large OARs were manually cropped to the region close to the target. Dose, however, was calculated on a whole OAR to ensure the validity of results.

For targets with different fractionation scheme (targets 8a-e), TRiP98 was modified to include option of specific dose fractions for specific target.

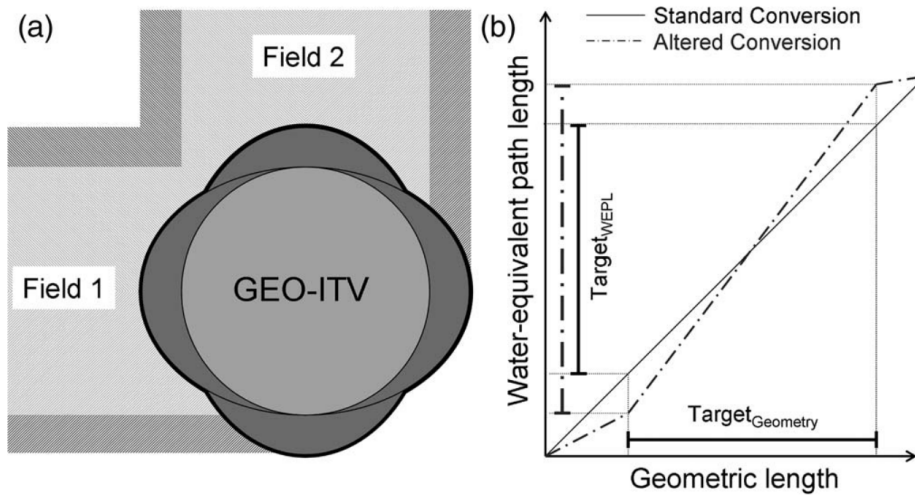


Figure 1.2: Schematic presentation of the ITV. (a) Dark gray ellipses show margins needed for specific fields to account for range changes in different motion states. When common target volume for two perpendicular fields is generated (this black contour) it creates unnecessary lateral extension of both fields, as shown by the dark gray entry channels. A solution is shown in (b). Rather than using standard, geometric margins, both fields use the same geometry, however the conversion of geometry to WEPL is altered for each field. The plot in (b) shows the standard (solid line) and an altered conversion (dashed-dotted line) for a beam passing a homogeneous CTV. The altered conversion increases the WEPL extent and thus implicitly increasing margins for a single field only. Figure taken from [Graeff et al., 2012]

1.2.4 Treatment planning

An isotropic margin of 3 mm was added to each CTV to account for uncertainties in treatment delivery. A WEPL-ITV was constructed on the CTV with margins for each individual field, which was then used either in optimization (ITV) or for raster setup (4Dopt). Due to large memory demands, targets in each lung were optimized separately.

The planning objective was 99% of each target volume should receive at least 100% of the planned dose ($D_{99\%} \geq 100\%$). Two dose limitation were used for OARs, as defined in the AAPM task group [Benedict et al., 2010]. The first limitation was a maximum dose to single voxel D_{Max} and the second a maximum dose deposited to a specific OAR volume $D_{Threshold}$. All limits are summarized in Table **appendix**.

After the optimization the 4D-dose was calculated for two motion periods (3.6 sec and 5.0 sec) and two starting phases (0° and 90°) as explained in Section ???. The relative biological effectiveness (RBE) was calculated with LEM IV [Elsaesser et al., 2010]. Alpha beta ratio of 6 and 2 was used in target and normal tissue, respectively.

Motion was mitigated by applying slice-by-slice rescanning to each plan. The number of rescans was limited by the number of particles in a single raster point, which should not be lower than 8000 due to the monitoring precision. The maximum number of rescans was limited to 20.

Detailed explanation of SBRT treatment planning is given in Section ??.

For patients 4 - 7 OAR dose could not be sufficiently reduced in optimization. It was necessary to add margins to the OAR and then subtract the OAR plus margins from the target. For SBRT the OAR plus margins was subtracted from PTV, which included 3 mm isotropic margins on a geometrical ITV. In PT geometrical ITV was not used, so in each of 10 motion states, OAR plus margins was subtracted from CTV plus 3 mm.

In the first try the OAR was included in optimization with different weights (w_{OAR} in Eq 1.1) and without any subtraction from target. If any 3D treatment plan after the optimization was acceptable, a 4D dose was calculated, where OAR and target dose were inspected. If the plan was rejected, the optimization was repeated but with OAR subtraction from target.

1.2.5 Dose escalation

A single fraction of 24 Gy could not be used in SBRT treatment for targets 4a, 7b and 8a-e due to OAR dose constraints. For these targets additional PT plans were generated with 1 x 24 Gy fractionation scheme, in order to estimate if PT could respect OAR constraints for these targets, while delivering 1 x 24 Gy.

1.2.6 Data evaluation

For target coverage comparison, the minimum dose in 99% of the target volume ($D_{99\%}$) was evaluated. D_{Max} and $D_{Threshold}$ were used in OAR dose comparison. D_{Max} and $D_{Threshold}$ were normalized to the respective limits in the fractionation scheme used, see Table ???. Additionally, the volume receiving 20% of the planned dose ($V_{20\%}$) was used to assess ipsilateral lung dose.

Paired t-tests were performed to compare the dose metrics mentioned between SBRT, ITV and 4Dopt. A p-value < 0.05 was considered significant.

1.3 Results

An example of different treatment plans for three patients are shown in Fig. 1.3.

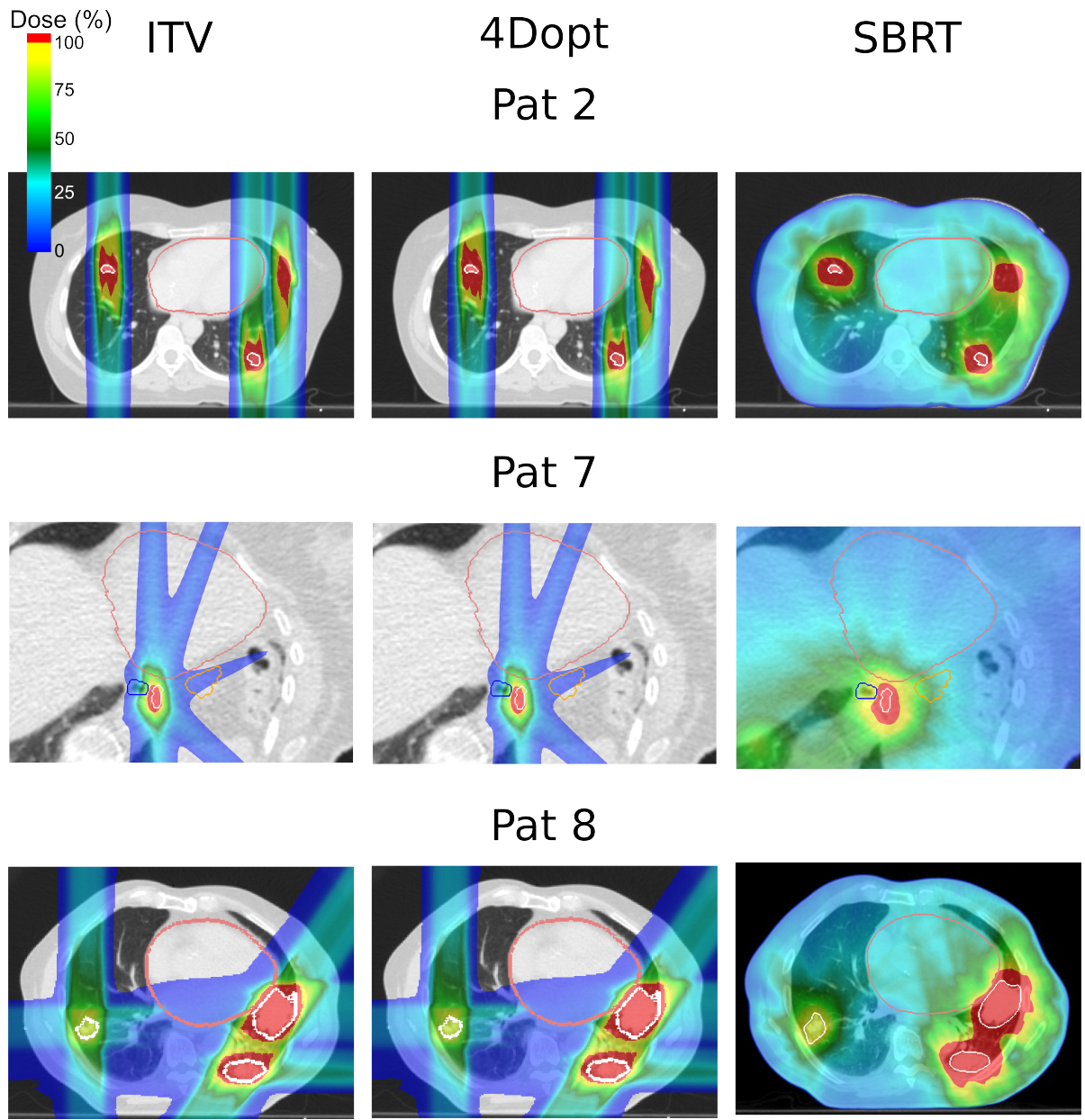


Figure 1.3: Treatment plans for ITV (left), 4Dopt (middle) and SBRT (right) for patients 2 (top), 7 (middle) and 8 (bottom). CTV, heart, esophagus and stomach contours are outlined in white, red, blue and orange, respectively. Patient 7 image is magnified to the target 7b location. Patient 2 has 5 disease sites with no OARs in target vicinity. Patient 7 had poor target coverage with PT due to large target motion and OAR proximity. A 1×24 Gy plan could be generated for patient 8 with PT, while SBRT was limited with heart dose and 2 targets were treated with 3×9 Gy, 2 with 1×20 Gy and one with 1×22 Gy.

1.3.1 Target Coverage

Results for CTV $D_{99\%}$ for all patients are shown in Table 1.2. All SBRT plans were approved by a physician, even though the prescription dose for patients 4 - 6 was not met due to an OAR proximity. Target 7b $D_{99\%}$ for PT was below prescription and SBRT delivered full dose. Average CTV $D_{99\%}$ was 97, 95 and 98% for ITV, 4Dopt and SBRT, respectively. There was a significant difference between ITV and 4Dopt and SBRT and 4Dopt.

Table 1.2: CTV $D_{99\%}$ for ITV, 4Dopt and SBRT for 8 patients. Results for ITV and 4Dopt are shown as median (range) across different motion types.

Patient	Target	CTV $D_{99\%}$ (%)		
		ITV	4Dopt	SBRT
1	a	101.0(101.0 - 101.0)	101.0(101.0 - 101.0)	100.0
	b	101.0(101.0 - 102.1)	101.0(101.0 - 101.0)	100.0
2	a	101.0(101.0 - 102.1)	100.0(99.0 - 102.1)	106.3
	b	102.1(102.1 - 102.1)	102.1(102.1 - 102.1)	103.1
	c	101.0(100.0 - 101.0)	101.6(101.0 - 102.1)	104.2
	d	102.1(101.0 - 102.1)	102.1(102.1 - 102.1)	107.3
	e	101.0(101.0 - 101.0)	101.0(101.0 - 102.1)	108.3
3	a	101.0(101.0 - 101.0)	101.0(101.0 - 101.0)	101.0
	b	98.4(97.9 - 99.0)	97.9(97.9 - 97.9)	102.1
4	a	65.3(63.9 - 69.4)	70.4(68.5 - 72.2)	66.7
	b	101.0(100.0 - 102.1)	100.5(100.0 - 102.1)	103.1
5	a	100.0(99.0 - 101.0)	100.0(100.0 - 100.0)	101.0
	b	101.6(100.0 - 102.1)	97.9(96.9 - 99.0)	101.0
	c	95.3(94.8 - 96.9)	94.3(92.7 - 94.8)	99.0
	d	99.0(97.9 - 99.0)	99.5(99.0 - 100.0)	94.8
6	a	89.1(88.5 - 90.6)	85.4(85.4 - 87.5)	69.8
	b	78.6(77.1 - 79.2)	72.4(71.9 - 72.9)	69.8
7	a	102.1(102.1 - 102.1)	99.0(99.0 - 99.0)	101.0
	b	83.9(82.1 - 85.7)	75.0(75.0 - 75.0)	100.0
8	a	100.0(100.0 - 100.9)	99.5(99.1 - 100.9)	105.6
	b	101.3(100.0 - 102.5)	100.0(100.0 - 101.3)	105.0
	c	100.0(99.1 - 100.0)	99.5(97.2 - 100.0)	106.5
	d	102.3(102.3 - 102.3)	89.8(89.8 - 90.9)	102.3
	e	102.5(102.5 - 102.5)	91.9(91.3 - 92.5)	101.3

1.3.2 Dose in OARs

D_{Max} and $D_{Threshold}$ for 8 OARs are shown in Table 1.3. Dose volume histograms (DVH) for patients 4, 6 and 7 are shown in Fig. 1.4. There was a significant difference between PT and SBRT in D_{Max} and $D_{Threshold}$ for heart, spinal cord, esophagus and aorta. No significant difference was

observed for D_{Max} and $D_{Threshold}$ in smaller airways. No significant difference was observed in dose to any OAR between different motion types or between ITV and 4Dopt. The overall OAR difference for patients between SBRT and ITV was significant, 17 (4 - 52)% and 27 (8 - 55)% of OAR limits for D_{Max} $D_{Threshold}$, respectively. The ipsilateral lung $V_{20\%}$ was 14.5(0.0 - 48.7), 14.4(0.0 - 43.7) and 29.8 (5.8 - 89.2)% for ITV, 4Dopt and SBRT, respectively. Both, ITV and 4DITV ipsilateral lung $V_{20\%}$ was significantly different from SBRT.

The margins used for OAR subtraction for PT and SBRT can be found in Table ??.

All treatment plans exceeded the D_{Max} limit for smaller airways in patients 4, 6 and 8 and for heart in patient 6. Additionally, SBRT esophagus and Heart D_{Max} limits were exceeded in patients 4 and 8, respectively.

Table 1.3: OAR D_{Max} , $D_{Threshold}$ and ipsilateral lung $V_{20\%}$ of all patients for ITV, 4Dopt and SBRT.

There was a significant difference between PT and SBRT for all OARs, except smaller airways' D_{Max} . D_{Max} and $D_{Threshold}$ doses are normalized to the corresponding OAR limits in the fractionation scheme used (see [Benedict et al., 2010]). Data is displayed as median (range).

OAR	ITV	4Dopt	SBRT
D_{Max} (%)			
heart	62.0(0.0 - 100.0)	59.5(0.0 - 97.0)	82.5(20.0 - 103.0)
spinalcord	13.0(0.0 - 48.0)	12.0(0.0 - 55.0)	60.0(21.0 - 79.0)
smaller airways	72.5(0.0 - 130.0)	71.0(0.0 - 117.0)	72.5(0.0 - 171.0)
esophagus	9.0(0.0 - 79.0)	8.0(0.0 - 99.0)	70.5(20.0 - 101.0)
aorta	17.5(8.0 - 61.0)	15.0(7.0 - 61.0)	45.0(15.0 - 74.0)
$D_{Threshold}$ (%)			
heart	15.5(0.0 - 59.0)	16.0(0.0 - 53.0)	62.5(19.0 - 98.0)
spinalcord	11.0(0.0 - 45.0)	10.0(0.0 - 53.0)	66.5(28.0 - 95.0)
smaller airways	28.0(0.0 - 97.0)	26.5(0.0 - 89.0)	68.5(0.0 - 99.0)
esophagus	1.0(0.0 - 17.0)	1.0(0.0 - 20.0)	49.0(17.0 - 99.0)
aorta	5.5(0.0 - 30.0)	5.5(0.0 - 28.0)	34.5(12.0 - 59.0)
$V_{20\%}$ (%)			
Ipsilateral lung	14.5(0.0 - 48.7)	14.4(0.0 - 43.7)	29.8(5.3 - 89.2)

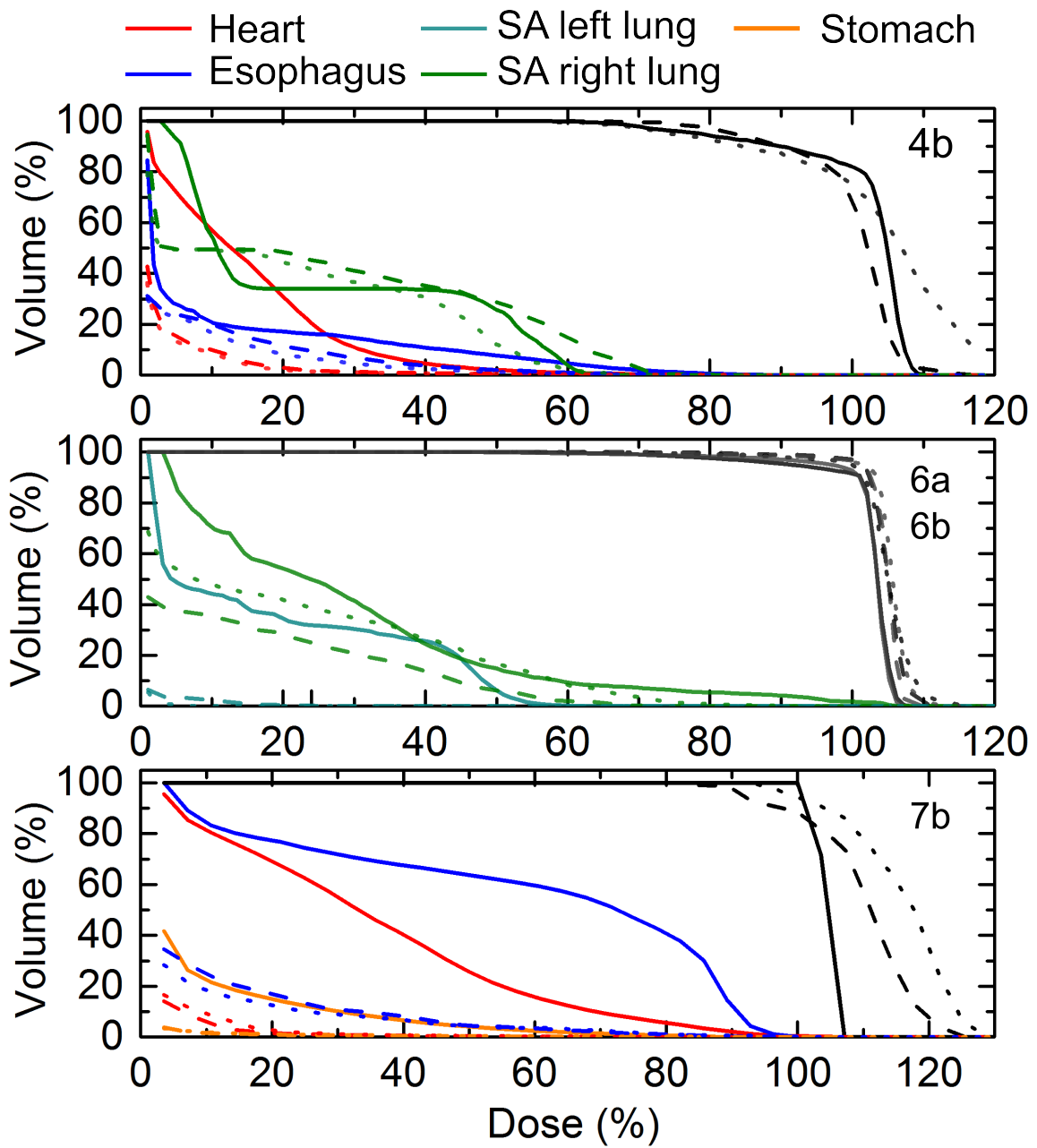


Figure 1.4: Dose volume histograms for targets 4b, 6a, 6b and 7b with relevant OARs. SBRT, ITV and 4DITV are represented by solid, dashed and dotted line, respectively. Targets are displayed in grayscale, while OAR colors are shown in legend. SA stands for smaller airways.

1.3.3 Dose escalation

With PT the 1×24 Gy fractionation scheme could be used for targets 8a-e, violating only D_{Max} for smaller airways (180%) and heart (110%). The SBRT for patient 8 was limited by heart D_{Max} and $D_{Threshold}$ which were 102% and 93%, respectively. The SBRT delivered a mean heart dose of 3 Gy in a single fraction (out of three), whereas PT's mean heart dose was 0.8 Gy. The difference in the heart dose can be seen in Fig 1.5.

For targets 4a and 7b the 1×24 Gy fractionation scheme could not be generated with PT. Either the target coverage was low ($CTV\ D_{99\%} < 50\%$) or esophagus D_{Max} and additionally stomach D_{Max} for target 7b were exceeded.

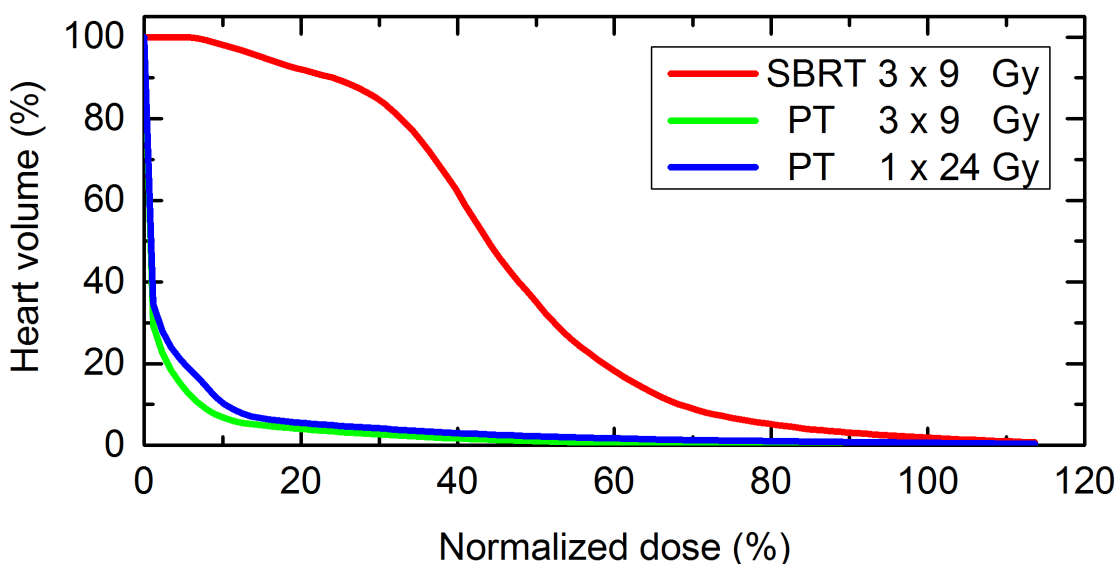


Figure 1.5: Dose volume histogram for Patient 8 heart dose. SBRT (red) plan was delivered in 3×9 Gy fractionation scheme. ITV PT plans were generated for the same fractionation scheme (green) and with dose escalation 1×24 scheme (blue). Dose was normalized to D_{Max} heart limit in respective fractionation scheme - 30 Gy in 3×9 Gy and 22 Gy in 1×24 Gy.

1.4 Summary and Discussion

Clinically valid SBRT plans have been compared to PT treatment plans for NSCLC patients with multiple metastases. To the best of our knowledge, this is the first study treating multiple NSCLC metastases with IMPT. A novel approach was used to handle multiple targets and combined with state of the art 4D IMPT treatment planning. Furthermore, 4D PT doses were calculated for different motion types.

PT on average delivered less dose to OARs, while still having comparable target coverage to SBRT. The most important difference was in heart dose, with $D_{Threshold}$ being on average 6 times lower in PT compared to SBRT. A recent trial, RTOG 0617, has shown, that a higher mortality rates could be attributed to higher heart dose for NSCLC patients [Bradley et al., 2015]. Furthermore, as seen in Table 1.3, the median $D_{Threshold}$ for all OARs is below 30% and $D_{Threshold}$ exceeds 90% in only one OAR in one patient. For SBRT $D_{Threshold}$ comes close to the limit in all OARs, except aorta. There was no need to include $D_{Threshold}$ in treatment planning, whereas it is imperative in SBRT.

For patients with complex geometry (4 - 8) PT maintained or even improved target coverage in most cases, while reducing doses to OARs. The exception was target 7b, where CTV $D_{99\%}$ was low (84% and 75% for ITV and 4Dopt, respectively), due to the D_{Max} constraints of esophagus and stomach. The large motion of target 7b (11.8 mm) and small target volume (0.4 cm^3) contributed to a poor PT plan, whereas SBRT was able to deliver full dose to the target and adhering to OAR constraints. This supports our claim in Chapter ?? that targets with larger volume would benefit most from PT. Furthermore, for small targets with large motion in OAR vicinity, PT generates worse plan than SBRT. It should be noted, however, that integral doses for all OARs are still lower for PT as seen in Fig 1.4. The only limitation for PT is usually the OAR's D_{Max} .

The biggest advantage of PT could be seen in Patient 8, where the fractionation scheme could be changed to $1 \times 24 \text{ Gy}$. The large total target volume of Patient 8 could be irradiated with less overall dose and hence significantly reduce dose to all OARs. Most notably, the heart dose, which was the limitation factor for SBRT. The difference of 2 Gy mean heart dose in a single fraction is tremendous and could influence the potential outcome for the specific patient. Again, this confirms our claim of PT benefit for large targets. Due to the OAR constraints of targets 4a and 7b, no fractionation escalation was possible with PT.

There was a small difference in average target coverage between ITV and 4Dopt. The most notable difference was in targets 8d and 8e, where CTV $D_{99\%}$ was 10% lower for 4Dopt. For this patient 4Dopt was done on a subset of 4D-CTstates, which may be inadequate due to the large motion of target 8e (17 mm). In a future study, the number of voxels included in optimization should be reduced, without loosing any target coverage. A possible solution would be an adap-

tive dose grid [Prall et al., 2016] There was no significant difference between ITV and 4Dopt in dose to OARs.

Even though PT deposits less dose to OARs with the same or even better target coverage, there is still room for improvement in PT 4D treatment planning. An implementation of multi-criteria objective planning should bring even better dose distribution and bring possibility to choose between trade-offs [Breedveld et al., 2007, Chen et al., 2010]. Additionally, multiple target optimization in PT would benefit from a shell around PT where dose would be minimized. Therefore excessive dose in healthy tissue would be further reduced. An introduction of a shell, however, would further enlarge the optimization problem, which is big already for complex geometries (patient 4 - 8). As mention, it might be possible to minimize the voxel number in optimization by an adaptive grid.

In Chapter ?? additional range margins to account for range uncertainties could be used in treatment planning, due to SFUD. Because we did not use field specific PTVs, it was not possible to include range uncertainties in our study. Instead of creating field specific PTVs to include range uncertainties, a solution was proposed to include uncertainties in the optimization process itself [Pflugfelder et al., 2008, Unkelbach et al., 2009, Fredriksson et al., 2011, Chen et al., 2012]. Chen et al. have implemented robust optimization in multi-criteria optimization as well [Chen et al., 2012]. Furthermore, in a recent treatment planning study by Liu et al. [Liu et al., 2016] a 4D robust optimization was demonstrated, with better results over 3D robust optimization for NSCLC patients. However, only breathing starting phase was used as an uncertainty, whereas different motion types should be considered. The disadvantage of 3D and 4D robust optimization is the enlargement of the optimization problem.

Patient 4 D_{Max} esophagus dose ranged over 1.3 Gy across different motion types in 4Dopt, showing the necessity of making treatment plans robust against motion uncertainty, especially in the hypo-fractionated regimen. Furthermore, OAR doses that are under the limits after optimization, may exceed them after calculating 4D dose. The ITV and 4Dopt approaches take into account range changes in different motion states, however they do not address interplay. This could be solved with a complete 4D optimization [Graeff et al., 2013], where a 4D raster treatment plan is generated and each motion state has a designated treatment plan.

Apart from 4D robust optimization, the effect of motion could be minimized by using other motion mitigation techniques, such as gating. Furthermore, gating could improve the target coverage, where the planned dose was not met. Gating, together with rescanning, has already been successfully implemented clinically for active beam scanning [Rossi, 2016, Mori et al., 2016] and it might be essential to use it in hypo-fractionated treatment of moving tumors [Richter et al., 2014].

A recent review showed good local control rates between 66 - 92% for patients treated with SBRT for in-field recurrent tumors [Amini et al., 2014]. However, there were grade 4 and 5 complications present, i.e. a study by Trovo et al showed grade 5 pneumonia in 6% of patients

treated [Trovo et al., 2014]. As shown in our study, PT delivers less dose to the OARs, ipsilateral lung in particular, and could hence reduce the number of treatment-related complications.

1.5 Conclusions

PT delivers less dose to OARs compared to SBRT in NSCLC patients with multiple disease sites, while maintaining target coverage. Patient with large total target volume could be irradiated with 1×24 Gy, whereas it could not with SBRT. There was a small difference between the two 4D treatment planning techniques.

Patients with multiple NSCLC disease site have a poor prognosis, with a median survival shorter than a year. Treatment with SBRT can prolong a patient life, however there is a 10% chance of death due to the severity of the treatment. PT could maintain the SBRT survival rate, while tremendously reducing treatment related side effects.

Bibliography

- [Amini et al., 2014] Amini, A., Yeh, N., Gaspar, L. E., Kavanagh, B., and Karam, S. D. (2014). Stereotactic body radiation therapy (sbrt) for lung cancer patients previously treated with conventional radiotherapy: a review. *Radiation Oncology*, 9(1):1–8.
- [Baumann et al., 2009] Baumann, P., Nyman, J., Hoyer, M., Wennberg, B., Gagliardi, G., Lax, I., Drugge, N., Ekberg, L., Friesland, S., Johansson, K. A., Lund, J. A., Morhed, E., Nilsson, K., Levin, N., Paludan, M., Sederholm, C., Traberg, A., Wittgren, L., and Lewensohn, R. (2009). Outcome in a prospective phase ii trial of medically inoperable stage i non-small-cell lung cancer patients treated with stereotactic body radiotherapy. *Journal of Clinical Oncology*, 27(20):3290–3296.
- [Benedict et al., 2010] Benedict, S. H., Yenice, K. M., Followill, D., Galvin, J. M., Hinson, W., Kavanagh, B., Keall, P., Lovelock, M., Meeks, S., Papiez, L., Purdie, T., Sadagopan, R., Schell, M. C., Salter, B., Schlesinger, D. J., Shiu, A. S., Solberg, T., Song, D. Y., Stieber, V., Timmerman, R., Tome, W. A., Verellen, D., Wang, L., and Yin, F. F. (2010). Stereotactic body radiation therapy: the report of aapm task group 101. *Medical Physics*, 37(8):4078–4101.
- [Bradley et al., 2015] Bradley, J. D., Paulus, R., Komaki, R., Masters, G., Blumenschein, G., Schild, S., Bogart, J., Hu, C., Forster, K., Magliocco, A., Kavadi, V., Garces, Y. I., Narayan, S., Iyengar, P., Robinson, C., Wynn, R. B., Koprowski, C., Meng, J., Beitler, J., Gaur, R., Curran, W. J., and Choy, H. (2015). Standard-dose versus high-dose conformal radiotherapy with concurrent and consolidation carboplatin plus paclitaxel with or without cetuximab for patients with stage iiia or iiib non-small-cell lung cancer (rtog 0617): a randomised, two-by-two factorial phase 3 study. *The Lancet Oncology*, 16(2):187–199.
- [Breedveld et al., 2007] Breedveld, S., Storchi, P. R. M., Keijzer, M., Heemink, A. W., and Heijmen, B. J. M. (2007). A novel approach to multi-criteria inverse planning for imrt. *Physics in Medicine and Biology*, 52(20):6339.
- [Chen et al., 2010] Chen, W., Craft, D., Madden, T. M., Zhang, K., Kooy, H. M., and Herman, G. T. (2010). A fast optimization algorithm for multicriteria intensity modulated proton therapy planning. *Med Phys*, 37(9):4938–4945.
- [Chen et al., 2012] Chen, W., Unkelbach, J., Trofimov, A., Madden, T., Kooy, H., Bortfeld, T., and Craft, D. (2012). Including robustness in multi-criteria optimization for intensity-modulated proton therapy. *Physics in Medicine and Biology*, 57(3):591–608.

- [Elsaesser et al., 2010] Elsaesser, T., Weyrather, W. K., Friedrich, T., Durante, M., Iancu, G., Krämer, M., Kragl, G., Brons, S., Winter, M., Weber, K. J., and Scholz, M. (2010). Quantification of the relative biological effectiveness for ion beam radiotherapy: direct experimental comparison of proton and carbon ion beams and a novel approach for treatment planning. *Int. J. Radiat. Oncol. Biol. Phys.*, 78(4):1177–1183.
- [Fakiris et al., 2009] Fakiris, A. J., McGarry, R. C., Yiannoutsos, C. T., Papiez, L., Willams, M., Henderson, M. A., and Timmerman, R. (2009). Stereotactic body radiation therapy for early-stage non-small-cell lung carcinoma: four-year results of a prospective phase ii study. *International Journal of Radiation Oncology*, 75(3):677–682.
- [Fredriksson et al., 2011] Fredriksson, A., Forsgren, A., and Hårdemark, B. (2011). Minimax optimization for handling range and setup uncertainties in proton therapy. *Medical Physics*, 38(3):1672–1684.
- [Graeff et al., 2012] Graeff, C., Durante, M., and Bert, C. (2012). Motion mitigation in intensity modulated particle therapy by internal target volumes covering range changes. *Medical Physics*, 39(10):6004–6013.
- [Graeff et al., 2013] Graeff, C., Lüchtenborg, R., Eley, J. G., Durante, M., and Bert, C. (2013). A 4d-optimization concept for scanned ion beam therapy. *Radiotherapy and Oncology*, 109(3):419 – 424.
- [Greco et al., 2011] Greco, C., Zelefsky, M. J., Lovelock, M., Fuks, Z., Hunt, M., Rosenzweig, K., Zatcky, J., Kim, B., and Yamada, Y. (2011). Predictors of local control after single-dose stereotactic image-guided intensity-modulated radiotherapy for extracranial metastases. *Int.J.Radiat.Oncol.Biol.Phys.*, 79(4):1151–1157.
- [Grutters et al., 2010] Grutters, J. P. C., Kessels, A. G. H., Pijls-Johannesma, M., Ruysscher, D., oore, M. A. ., and Lambin, P. (2010). Comparison of the effectiveness of radiotherapy with photons, protons and carbon-ions for non-small cell lung cancer: A meta-analysis. *Radiotherapy and Oncology*, 95(1):32–40.
- [Iyengar et al., 2014] Iyengar, P., Kavanagh, B. D., Wardak, Z., Smith, I., Ahn, C., Gerber, D. E., Dowell, J., Hughes, R., Camidge, D. R., Gaspar, L. E., Doebele, R. C., Bunn, P. A., Choy, H., and Timmerman, R. (2014). Phase ii trial of stereotactic body radiation therapy combined with erlotinib for patients with limited but progressive metastatic non-small-cell lung cancer. *J.Clin.Oncol.*, 32(34):3824–3854.
- [Krämer and Scholz, 2000] Krämer, M. and Scholz, M. (2000). Treatment planning for heavy-ion radiotherapy: calculation and optimization of biologically effective dose. *Phys. Med. Biol.*, 45(11):3319–3330.

- [Liu et al., 2016] Liu, W., Schild, S. E., Chang, J. Y., Liao, Z., Chang, Y.-H., Wen, Z., Shen, J., Stoker, J. B., Ding, X., Hu, Y., Sahoo, N., Herman, M. G., Vargas, C., Keole, S., Wong, W., and Bues, M. (2016). Exploratory study of 4d versus 3d robust optimization in intensity modulated proton therapy for lung cancer. *International Journal of Radiation Oncology*, 95(1):523–533.
- [Mori et al., 2016] Mori, S., Karube, M., Shirai, T., Tajiri, M., Takekoshi, T., Miki, K., Shiraishi, Y., Tanimoto, K., Shibayama, K., Yasuda, S., Yamamoto, N., Yamada, S., Tsuji, H., Noda, K., and Kamada, T. (2016). Carbon-ion pencil beam scanning treatment with gated markerless tumor tracking: An analysis of positional accuracy. *International Journal of Radiation Oncology*, 95(1):258–266.
- [Pflugfelder et al., 2008] Pflugfelder, D., Wilkens, J. J., and Oelfke, U. (2008). Worst case optimization: a method to account for uncertainties in the optimization of intensity modulated proton therapy. *Phys Med Biol*, 53(6):1689–1700.
- [Prall et al., 2016] Prall, M., Hild, S., Anderle, K., and Graeff, C. (2016). Treatment planning with an adaptive dose grid. In *Abstract Book PTCOG 55*.
- [Ramalingam and Belani, 2008] Ramalingam, S. and Belani, C. (2008). Systemic chemotherapy for advanced non-small cell lung cancer: Recent advances and future directions. *The Oncologist*, 13(suppl 1):5–13.
- [Richter et al., 2014] Richter, D., Graeff, C., Jakel, O., Combs, S. E., Durante, M., and Bert, C. (2014). Residual motion mitigation in scanned carbon ion beam therapy of liver tumors using enlarged pencil beam overlap. *Radiotherapy and Oncology*, 113(2):290–295.
- [Richter et al., 2013] Richter, D., Schwarzkopf, A., Trautmann, J., Kramer, M., Durante, M., Jakel, O., and Bert, C. (2013). Upgrade and benchmarking of a 4d treatment planning system for scanned ion beam therapy. *Medical Physics*, 40(5):051722.
- [Rossi, 2016] Rossi, S. (2016). The national centre for oncological hadrontherapy (cnao): Status and perspectives. *Physica Medica: European Journal of Medical Physics*, 31(4):333–351.
- [Rusthoven et al., 2009] Rusthoven, K. E., Kavanagh, B. D., Burri, S. H., Chen, C., Cardenes, H., Chidel, M. A., Pugh, T. J., Kane, M., Gaspar, L. E., and Schefter, T. E. (2009). Multi-institutional phase i/ii trial of stereotactic body radiation therapy for lung metastases. *Journal of Clinical Oncology*, 27(10):1579–1584.
- [Salama et al., 2012] Salama, J. K., Hasselle, M. D., Chmura, S. J., Malik, R., Mehta, N., Yenice, K. M., Villaflor, V. M., Stadler, W. M., Hoffman, P. C., Cohen, E. E. W., Connell, P. P., Haraf, D. J., Vokes, E. E., Hellman, S., and Weichselbaum, R. R. (2012). Stereotactic body radiotherapy for multisite extracranial oligometastases. *Cancer*, 118(11):2962–2970.

- [Siegel et al., 2014] Siegel, R., Ma, J., Zou, Z., and Jemal, A. (2014). Cancer statistics, 2014. *CA: A Cancer Journal for Clinicians*, 64(1):9–29.
- [Socinski et al., 2013] Socinski, M. A., Evans, T., Gettinger, S., Hensing, T. A., Sequist, L. V., Ireland, B., and Stinchcombe, T. E. (2013). Treatment of stage {IV} non-small cell lung cancer: Diagnosis and management of lung cancer, 3rd ed: American college of chest physicians evidence-based clinical practice guidelines. *Chest*, 143(5, Supplement):e341S – e368S.
- [Trovo et al., 2014] Trovo, M., Minatel, E., Durofil, E., Polasel, J., Avanzo, M., Baresic, T., Bearz, A., Del Conte, A., Franchin, G., Gobitti, C., Rumeileh, I. A., and Trovo, M. G. (2014). Stereotactic body radiation therapy for re-irradiation of persistent or recurrent non-small cell lung cancer. *Int J Radiat Oncol Biol Phys*, 88.
- [Tsujii and Kamada, 2012] Tsujii, H. and Kamada, T. (2012). A review of update clinical results of carbon ion radiotherapy. *Jpn.J.Clin.Oncol.*, 42(8):670–685.
- [Unkelbach et al., 2009] Unkelbach, J., Bortfeld, T., Martin, B. C., and Soukup, M. (2009). Reducing the sensitivity of impt treatment plans to setup errors and range uncertainties via probabilistic treatment planning. *Med Phys*, 36(1):149–163. 074812MPH[PII].
- [Villaruz et al., 2012] Villaruz, L. C., Kubicek, G. J., and Socinski, M. A. (2012). Management of non-small cell lung cancer with oligometastasis. *Current Oncology Reports*, 14(4):333–341.